Evidence for another low-temperature phase transition in tetragonal $Pb(Zr_xTi_{1-x})O_3$ ($x=0.515,0.520$)

Ragini, S. K. Mishra, and Dhananjai Pandey
School of Materials Science and Technology, Institute of Technology, Banaras Hindu University, Varanasi-221005, India

Herman Lemmens and G. Van Tendeloo
Electron Microscopy for Materials Research, University of Antwerp, Groenenborgerlaan, 171, B-2020, Antwerp, Belgium

(Received 4 May 2000; revised manuscript received 2 February 2001; published 29 June 2001)

Results of dielectric and resonance frequency (f_r) measurements below room temperature are presented for $Pb(Zr_xTi_{1-x})O_3$, $x=0.515$ and 0.520. It is shown that the temperature coefficient of f_r changes sign from negative to positive around 210 and 265 K for $x=0.520$ and 200 and 260 K for $x=0.515$. Anomalies in the real part of the dielectric constant (ε') are observed around the same temperatures at which the temperature coefficient of f_r changes sign because of the electrostrictive coupling between the elastic and dielectric responses. Low-temperature powder x-ray-diffraction (XRD) data, however, reveal only one transition from the tetragonal to monoclinic phase similar to that reported by Noheda *et al.* [Phys. Rev. B, **61**, 8687 (2000)]. Electron-diffraction data, on the other hand, reveal yet another structural transition at lower temperatures corresponding to the second anomaly in the ε' vs T and f_r vs T curves. This second transition is shown to be a cell-doubling transition not observed by Noheda *et al.* in their XRD studies. The observation of superlattice reflections raises doubts about the correctness of the *Cm* space group proposed by Noheda *et al.* for the monoclinic phase of $Pb(Zr_xTi_{1-x})O_3$ below the second transition temperature.

DOI: 10.1103/PhysRevB.64.054101 PACS number(s): 77.84.Dy, 77.80.Bh

I. INTRODUCTION

Recent years have witnessed a revival of interest in understanding the stability of various phases in the technologically important $Pb(Zr_xTi_{1-x})O_3$ (PZT) ceramics.[1–9] The phase diagram of PZT shows[10] a morphotropic phase boundary (MPB) which separates the ferroelectric tetragonal (F_T) and rhombohedral (F_R) phase fields on the Ti- and Zr-rich sides, respectively. This phase boundary is of immense technological importance since the dielectric constant (ε'), piezoelectric constant (d_{ij}), and electromechanical coupling coefficient (k) all show maximum response in the vicinity of the MPB.[10] However, the reason for this enhanced electromechanical response near the MPB is still not clear. Based on the concepts of the thermodynamics of solutions, it was proposed[11,12] in early literature that the stable state of the system at the MPB should be a mixture of F_T and F_R phases. The range of composition (Δx) over which such a coexistence should occur will be decided by the intersection of the free energy (ΔG) versus x curves for the F_T and F_R phases.[11,12] It was argued[13] that the availability of 14 possible domain configurations (six for F_T and eight for F_R phases) due to the phase coexistence improves the alignment of polar direction in ceramic specimens on the application of an intense dc electric field. This enhanced poling efficiency was regarded to be responsible for the high electromechanical response of PZT ceramics for the MPB composition. The coexistence of the two phases over a composition range $\Delta x \approx 0.15$ in PZT samples prepared by a solid-state reaction method was taken[11] as evidence of this model, even though Δx is now known to depend on the method of sample preparation.[14]

However, doubts have been raised about this model of phase coexistence at the MPB by Kakegawa and co-workers,[15,16] who attributed the phase coexistence to compositional fluctuations in samples prepared by the solid-state route. However, even in highly homogeneous PZT samples prepared by a semiwet route,[17] the authors of Ref. 2 showed that the F_T and F_R phases coexist for $x=0.525$, while pure F_T and F_R phases are stable for $x \leqslant 0.520$ and $x \geqslant 0.530$ compositions, respectively. This method of preparation gives the narrowest composition width ($\Delta x \approx 0.01$) for phase coexistence in the MPB region. Using the resonance frequency (f_r),[1,3] the planar electromechanical coupling coefficient (k_p),[1,3] and x-ray-diffraction[1,2] (XRD) measurements as a function of temperature, Mishra and co-workers[1,3] established the following sequence of phase transitions near the MPB: F_T to P_c (paraelectric cubic phase) for $x \leqslant 0.520$, $F_T + F_R \rightarrow F_T \rightarrow P_c$ for $x=0.525$, $F_R \rightarrow F_R + F_T \rightarrow F_T \rightarrow P_c$ for $0.530 \leqslant x \leqslant 0.545$, and $F_R \rightarrow P_c$ for $x \geqslant 0.550$ on successively increasing the temperatures. These results suggest that the phase coexistence at the MPB ($x=0.525$) is due to a first-order phase transition between the low-temperature rhombohedral (stable below room temperature) and higher-temperature tetragonal phases, since even the pure F_R phase passed through a two-phase region consisting of F_R and F_T phases before transforming fully into the F_T phase. This model of phase coexistence, in which only one of the phases is a thermodynamically stable phase, whereas the other one is in the metastable state, is different from the phase coexistence model of Refs. 11 and 12 where the free energy is minimum for the phase coexistence since a common tangent can be drawn to the intersecting ΔG vs x curves for the F_T and F_R phases. Mishra and Pandey[3] also proposed a phase diagram showing the phase coexistence region near the MPB. The work of Mishra and co-workers[1,3] revealed that

the electromechanical response of PZT ceramics containing the coexistence of F_T and F_R phases ($x=0.525$) increases with temperature due to decreasing F_R phase content, and reaches a maximum when the structure is purely tetragonal (F_T). This was the first clinching evidence against the decades old belief[13] that the phase coexistence is responsible for the maximum electromechanical response near the MPB compositions. Mishra and co-workers[1,3] proposed that the enhanced electromechanical response near the MPB compositions is linked with the instability in the vicinity of the *R* to *T* phase transition. The first evidence for such an instability was found by Thapa[18] in our laboratory, who observed a dielectric anomaly in tetragonal PZT with $x=0.520$ just below the room temperature. Recently, Noheda and co-workers[4,5] presented XRD evidence to show that there is a tetragonal to monoclinic phase transition in PZT around 250 and 200 K for $x=0.520$ and 0.50, respectively.

In this paper, we present the results of low-temperature dielectric, resonance frequency, x-ray-diffraction, and electron-diffraction studies on the tetragonal to monoclinic transition in PZT near the MPB. The dielectric constant (ε') and resonance frequency (f_r) measurements show that tetragonal PZT ($x=0.515$ and 0.520) undergoes two low-temperature phase transitions, whereas low-temperature XRD studies indicate only one transition. Our XRD results confirm that the first anomaly in $\varepsilon'(T)$ and $f_r(T)$ is due to the tetragonal to monoclinic transition reported by Noheda *et al.*[4] The second anomaly observed by us is due to a cell-doubling transition, leading to the appearance of weak superlattice reflections which are not seen in the powder XRD patterns but are clearly discernible on the selected area electron diffraction patterns. The origin of cell-doubling transition in the monoclinic phase is discussed in relation to a similar transition in the F_R phase.[19,20]

II. EXPERIMENT

A. Sample preparation

In order to bring out the subtle features of the PZT phase diagram near the morphotropic phase boundary, such as very weak anomalies in the dielectric constant at the monoclinic to tetragonal phase transition temperature, it is absolutely essential to have samples of exceptionally high quality in terms of chemical homogeneity. There are two sources of chemical heterogeneities in PZT: (i) the loss of PbO due to its high vapor pressure above 1023 K, and (ii) nonuniform mixing of Zr^{4+} and Ti^{4+} at the B^{4+} site of the ABO_3 structure. In the conventional solid-state reaction technique, requirement of high calcination temperatures, such as 1173 K used by Guo *et al.*,[8] may promote PbO loss. To minimize the PbO loss during sintering, a PbO source is commonly used.[8] However, an excess of PbO may also promote phase coexistence, as shown recently by Kakegawa *et al.*[16] The solid-state thermochemical reaction in this method takes place in more than one step. At the early stages of reaction, $PbTiO_3$ is formed first at a comparatively lower temperature, which then reacts with ZrO_2 to give a PZT solid solution at higher temperatures. This multistep reaction mechanism[21] remains as intrinsic source of nonuniform distribution of Zr^{4+} and Ti^{4+} in the solid-state reaction method because the driving force, mainly coming from the entropy of mixing, for Zr^{4+} diffusion at the calcination temperature is rather small.

Our samples were prepared by a semiwet route[17] in which submicron size single-phase PZT powders are obtained at 973 K in 6 h in a single-step reaction in a mixture of $PbCO_3$ and $(Zr_xTi_{1-x})O_2$ solid solution precursor. Use of a low calcination temperature ensures good Pb^{2+} stoichiometry. The unit-cell level mixing of Zr^{4+} and Ti^{4+} is pre-ensured in each precursor particle of $(Zr_xTi_{1-x})O_2$ in the ratio desired for the final PZT composition,[14] since $(Zr_xTi_{1-x})O_2$ has been obtained from the thermal decomposition of chemically coprecipitated $(Zr_xTi_{1-x})(OH)_4$ powders, and also the fact that it is a solid solution.

The PZT powders thus obtained were remilled and then pressed into pellets of 13-mm diameter and 1.5-mm thickness at an optimum load of 100 kN. The final sintering was carried out at 1373 K for 6 h in a PbO atmosphere, without adding any extra PbO, as usually done in the conventional solid-state reaction route. The weight loss due to possible PbO escape was less than 0.1%, and the sintered densities were in excess of 97% of the theoretical density. The x-ray line profile analysis of the sintered powders has confirmed[17] excellent chemical homogeneity. These powders show[2,17] a pure tetragonal structure for $x<0.520$, and a rhombohedral structure for $x\geqslant 0.530$ with an extremely sharp MPB region of $\Delta x\approx 0.01$.

B. Data collection

For electrical measurements, fired-on (firing temperature 773 K, duration: 30 min) silver electrodes were applied on both sides of the pellets. The samples were poled at a field of about 20 kV/cm at 373 K for 50 min. The dielectric and resonance frequency measurements were carried out on poled samples using impedance analyzers (Solartron model SI-1260 and HP model 4192). The sample temperature was varied with an accuracy of about ± 1 K below room temperature.

For XRD measurements, pellets were crushed to fine powders and annealed overnight at 773 K to get rid of strains introduced during crushing. A Rigaku 12-kW Cu-rotating anode was used as a source of x-ray ($Cu\,K\alpha$ radiation). Powder XRD data were collected on a Rigaku powder diffractometer based on Bragg-Brentano geometry. A Ge crystal monochrometer was used in the diffraction beam. For low-temperature studies, the powder sample was mounted on the cold finger of a Rigaku low-temperature attachment capable of going up to liquid-nitrogen temperature. The temperature was controlled manually within ± 2 K.

Transmission electron microscope (TEM) studies were carried out using a Philips model CM20 with Gatan liquid-nitrogen-cooling stage. The ion-milled samples were used for the TEM examinations.

III. RESULTS AND DISCUSSION

The elastic constant of normal solids, which expand on heating, is known to decrease with increasing temperature.

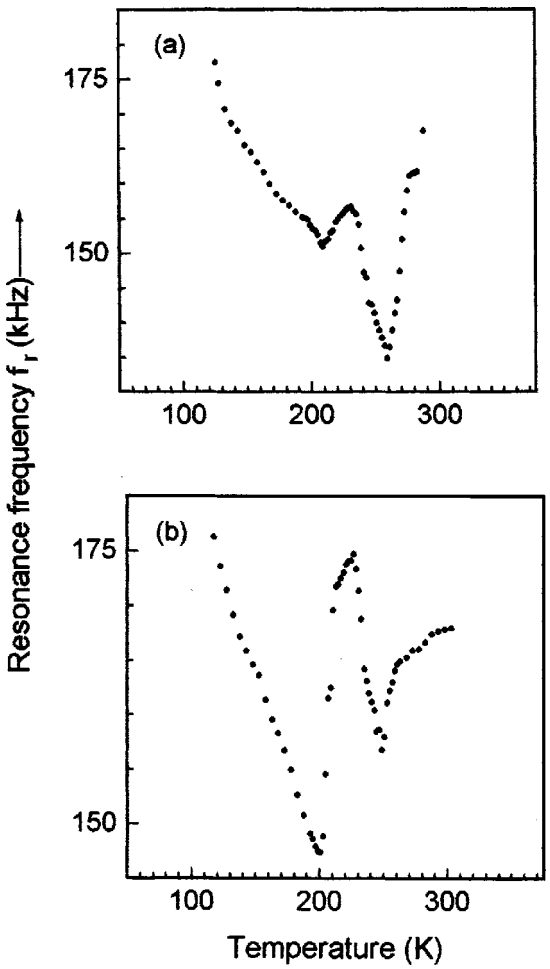

FIG. 1. Temperature variation of the resonance frequency (f_r) of poled $Pb(Zr_xTi_{1-x})O_3$ ceramics: (a) $x=0.520$; (b) $x=0.515$ showing two anomalies.

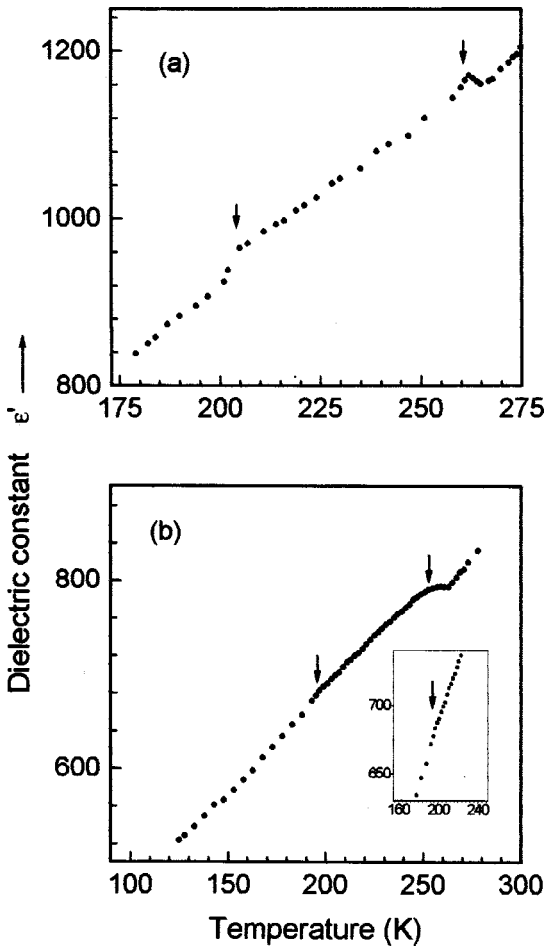

FIG. 2. Temperature variation of the real (ε') part of the dielectric constant for $Pb(Zr_xTi_{1-x})O_3$ ceramics with (a) $x=0.520$ (poled) and (b) $x=0.515$ (unpoled) showing two anomalies.

Since f_r varies as the square root of the elastic constant, it should also decrease with increasing temperature, i.e., the temperature coefficient of f_r (TCF) should be negative. This indeed is observed for the rhombohedral compositions ($x \geqslant 0.530$) outside the MPB region, as already shown elsewhere by Mishra and Pandey,[3] f_r, can, however, show an anomalous temperature dependence, i.e., a positive temperature coefficient, in the vicinity of a structural phase transition due to elastic instabilities. Figures 1(a) and 1(b) depict the variation of the resonance frequency (f_r) with temperature below the room temperature for poled tetragonal PZT ceramic samples with $x=0.520$ and 0.515. It is evident from Fig. 1(a) that the TCF is positive below the room temperature up to 261 K. The positive TCF in this temperature range is anomalous and is a signature of an impending structural phase transition which occurs below 261 K since the sign of TCF becomes negative below this temperature. The TCF again changes sign and becomes positive below 231 K, signaling the onset of yet another phase transition occurring at 209 K below which the negative sign of TCF is restored. For $x=0.515$ also, one finds that the sign of TCF changes twice below the room temperature, first at 249 K and subsequently around 201 K as shown in Fig. 1(b).

The temperature around which the sign of TCF changes, one also observes anomalies in the dielectric constant (ε') because of the electrostrictive coupling between the elastic and dielectric responses. This is illustrated in Figs. 2(a) and 2(b) for $x=0.520$ and 0.515. For $x=0.520$, there are two anomalies in $\varepsilon'(T)$ at 205 and 262 K. These temperatures are in fairly good agreement with the temperatures (209 and 261 K) around which the TCF changes its sign. For $x=0.515$, also, there are two anomalies in $\varepsilon'(T)$ as revealed by the change of slope around 197 and 253 K in Fig. 2(b). Thus the dielectric studies also suggest the existence of two low-temperature phase transitions in the tetragonal PZT compositions close to the MPB. It may be noted that the two anomalies in $\varepsilon'(T)$ are superimposed on a quasilinearly increasing $\varepsilon'(T)$ background which continues beyond room temperature until it leads to a peak corresponding to the tetragonal to cubic phase transition, as already shown elsewhere.[3] The observation of the low-temperature anomalies in $f_r(T)$ as well as $\varepsilon'(T)$ implies the interaction of the acoustic and optical phonons.

Unlike the $f_r(T)$ and $\varepsilon'(T)$ measurments, XRD studies reveal only one structural phase transition similar to that reported by Noheda *et al.*[4] This is illustrated in Fig. 3 which depicts the temperature evolution of 200, 220, and 222

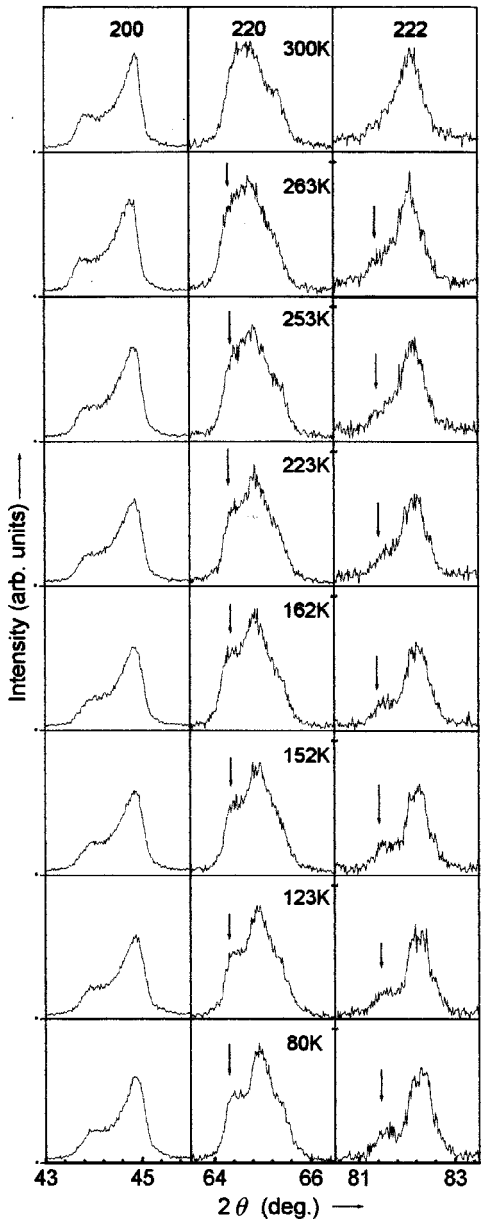

FIG. 3. Evolution of the XRD profiles as a function of temperature showing the tetragonal to monoclinic phase transition for $Pb(Zr_{0.52}Ti_{0.48})O_3$. The profiles shown correspond to the 200, 220 and 222 pseudocubic indices.

pseudocubic reflections for $x=0.520$. The pseudocubic 200 and 220 reflections form a doublet (002 and 200, 202 and 220), while 222 is a singlet for pure tetragonal phase as can be seen from the XRD profiles at 300 K in Fig. 3. For the rhombohedral structure, the 200 pseudocubic reflection is a singlet, while the 220 and 222 reflections become doublets. The fact that for $T \leqslant 263\,\mathrm{K}$, the 200 pseudocubic peak is a doublet, while 220 and 222 pseudocubic peaks split into triplets, suggests that the structure at $T \leqslant 263\,\mathrm{K}$ is neither tetragonal nor rhombohedral. The third reflection in the pseudocubic 222 peak is visible in the lower-temperature plots in Fig. 3. Following Noheda *et al.*,[4] we propose that the structure of this phase is monoclinic with space group *Cm*. It may be mentioned that for the monoclinic phase, the pseudocubic

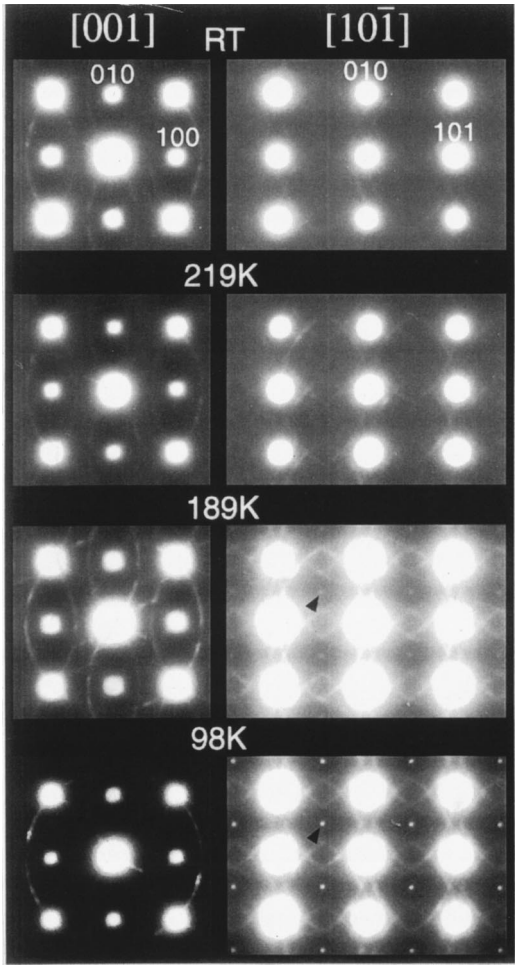

FIG. 4. The evolution of [001] and $[10\bar{1}]$ zone-axis-selected area electron-diffraction patterns with temperature. The appearance of superlattice reflections (marked with arrow) with pseudocubic indices $1/2\{h,k,l\}$ in the patterns at 189 and 98 K are due to the cell-doubling transition.

220 reflection consists of four peaks of which only three are resolved in the low-temperature plots in Fig. 3. The structural phase transition temperature of about 263 K, based on the appearance of the new peaks marked with arrows in Fig. 3, coincides with the first low temperature anomaly in $f_r(T)$ and $\varepsilon'(T)$ plots shown in Figs. 1(a) and 2(a) respectively. However, there is no signature of any further change of structure in Fig. 3 on lowering the temperature below 263 K, corresponding to the second anomaly in the $f_r(T)$ and $\varepsilon'(T)$ data in Figs. 1(a) and 2(a).

Figure 4 depicts the temperature evolution of [001] and $[10\bar{1}]$ zone-selected area electron-diffraction (SAD) patterns for $x=0.515$. The behavior of the $x=0.520$ sample also follows the same trend. The monoclinic distortions taking place below 263 K, observed in the XRD profiles, are too small to be detected in the SAD patterns for both the zones. The [001] zone pattern remains unchanged, as can be seen from Fig. 4. However, in the $[10\bar{1}]$ zone patterns, weak superlattice reflections with pseudocubic indices of the type $\frac{1}{2}\{h,k,l\}$ with $h,k,l=2n+1$ appear at low temperatures as shown for

189 and 98 K in Fig. 4. These superlattice reflections are not present in the SAD patterns corresponding to 219 K and room temperature. The intensity of the superlattice reflections increases with decreasing temperature, as can be seen from a comparison of the SAD patterns corresponding to 189 and 98 K. The appearance of these superlattice reflections clearly suggests that the pesudocubic unit cell is doubled somewhere between 219 and 189 K. Since the sign of TCF also changes at 201 K for $x=0.515$, the second anomaly in the $f_r(T)$ and $\varepsilon'(T)$ plots is due to a cell-doubling transition. The structure of this phase with a doubled cell also seems to be monoclinic or at least pseudomonoclinic, since all the reflections in the XRD patterns below the second transition temperature could be indexed with respect to a monoclinic cell. The monoclinic unit cell dimensions of the lowest temperature phase F_M^{LT} are related to those of the higher temperature phase F_M^{HT} as $a_{\mathrm{LT}}=a_{\mathrm{HT}}$, $b_{\mathrm{LT}}=b_{\mathrm{HT}}$, and $c_{\mathrm{LT}}=2c_{\mathrm{HT}}$. Thus, while the XRD results confirm that the first transition is from the tetragonal to a monoclinic (F_M^{HT}) phase, the electron-diffraction studies provide structural evidence for a second transition (i.e., an F_M^{HT} to F_M^{LT} phase) which is a cell-doubling transition. The superlattice reflections observed by us cannot be accounted for in terms of the *Cm* space group proposed by Noheda *et al.*[5] for PZT with $x=0.52$ at $T=20$ K (which is well below the second transition temperature for this composition).

The $\frac{1}{2}\{h,k,l\}$, $h,k,l=2n+1$ type superlattice reflections observed below the second transition can arise either due to antiparallel displacements of heavy ions like Pb^{2+} and Zr^{4+}/Ti^{4+},[20] or due to antiphase rotation of the oxygen octahedra in the neighboring unit cells.[22] The fact that the superlattice reflections due to the second transition are not observed in the XRD patterns seems to suggest that their origin lies in the antiphase rotation of oxygen octahedra. Such antiphase rotations mainly affect the oxygen positions for which the x-ray diffraction has a low sensitivity. Neutron-diffraction data may probably reveal the presence of these superlattice reflections.

A similar cell-doubling transition is known to occur for the rhombohedral phase of PZT on the Zr-rich side of MPB, as shown by several workers using neutron,[19] and electron-diffraction[20] data. The high-temperature rhombohedral phase (F_R^{HT}) transforms into a low-temperature rhombohedral (F_R^{LT}) phase in which the oxygen octahedra are rotated in an antiphase manner about the polar [111] axis, leading to a doubling of the pseudocubic cell. Anomalies in the TCF (Ref. 23) and dielectric constant[19] were reported at the F_R^{HT} to F_R^{LT} transition similar to what we have observed for the F_M^{HT} to F_M^{LT} phase transition. However, there is some controversy about the origin of the superlattice reflections observed in the electron-diffraction patterns of the F_R^{LT} phase. Superlattice reflections with $\frac{1}{2}\{h,k,l\}$-type pseudocubic indices with $h\neq k\neq l$, h, k, and $l=2n+1$ (denoted as R_2 type in Ref. 20) are consistent with an a^-,a^-,a^- tilt system[22] for the F_R^{LT} phase, and are also present in the neutron-diffraction patterns. The corresponding octahedral tilts arise through the condensation of the R point ($q=\frac{1}{2},\frac{1}{2},\frac{1}{2}$) phonons at the Brillouin-zone boundary. In the electron-diffraction patterns, one also observes[20,24] $\frac{1}{2}\{h,k,l\}$-type reflections with $h=k=l$ (denoted as R_1 type in Ref. 20) whose origin cannot be accounted for in terms of the octahedral tilts.[20] The origin of $1/2\{h,k,l\}$ with $h=k=l(=2n+1)$ type reflections was explained[20] by postulating antiparallel displacement of Pb^{2+} ions. The fact that these R_1-type superlattice reflections occur uniquely in electron (and not neutron or x-ray) diffraction suggests that the structures responsible for them are caused by surface effects in the TEM specimens.[20] The superlattice reflections observed by us are of R_1 type as well as R_2 type. In close analogy with the F_R^{LT} phase, the R_2-type superlattice reflections observed by us in the F_M^{LT} phase are clearly indicative of octahedral tilts, but the R_1-type reflections could well be due to the surface effects in thin TEM specimens. This needs to be verified in any future neutron-diffraction study.

IV. CONCLUSIONS

The MPB for PZT samples prepared by the semiwet route lies in the composition range $0.520<x<0.530$ and its intrinsic width is very narrow ($\Delta x\leqslant 0.01$). The temperature variation of the dielectric constant and resonance frequency for tetragonal compositions ($x=0.515$ and 0.520) close to the MPB shows that there are two low-temperature phase transitions. Low-temperature XRD data confirm that the first transition is from the tetragonal (space group $P4mm$) to a monoclinic F_M^{HT} (space group *Cm*) phase similar to that reported by Noheda *et al.*[4] The second transition is a cell-doubling transition. The structure of this phase (F_M^{LT}) with a doubled cell also seems to be monoclinic or at least pseudomonoclinic since all the reflections in the XRD pattern below the second transition temperature could be indexed with respect to a monoclinic cell. However, the observed superlattice reflections of R_2 type in the F_M^{LT} phase, due to antiphase rotation of the oxygen octahedra, cannot be accounted for in terms of the *Cm* space group assigned by Noheda *et al.* for the low-temperature phase of PZT with $x=0.520$ at 20 K. The assignment of the correct space group for the lowest temperature phase of PZT with $x=0.50$, 0.515, and 0.520 has to await the results of neutron diffraction studies which are currently underway.

ACKNOWLEDGMENTS

One of us (D. P.) is grateful to Professor T. V. Ramakrishnan for providing us copies of recent PZT papers. S. K. M. is grateful to the Council of Scientific and Industrial Research (CSIR) of India for the award of a Research Associateship. This work was partially supported by Inter University Consortium for the Department of Atomic Energy Facilities (IUC-DAEF) of the Government of India. We thank Dr. N. P. Lalla, IUC-DAEF, Indore Center for his help in the low-temperature XRD data collection.

[1] S. K. Mishra, A. P. Singh, and D. Pandey, Appl. Phys. Lett. **69**, 1707 (1996).
[2] S. K. Mishra, A. P. Singh, and D. Pandey, Philos. Mag. B **76**, 213 (1997).
[3] S. K. Mishra and D. Pandey, Philos. Mag. B **76**, 227 (1997).
[4] B. Noheda, D. E. Cox, G. Shirane, J. A. Gonzalo, L. E. Cross, and S. E. Park, Appl. Phys. Lett. **74**, 2059 (1999).
[5] B. Noheda, J. A. Gonzalo, L. E. Cross, R. Guo, S. E. Park, D. E. Cox, and G. Shirane, Phys. Rev. B **61**, 8687 (2000).
[6] L. Bellaiche, A. Garcia, and D. Vanderbilt, Phys. Rev. Lett. **84**, 5427 (2000).
[7] A. G. Sonze Filho, K. C. V. Lima, A. P. Ayala, I. Guedes, P. T. C. Freire, J. Mendes Filho, E. B. Araujo, and J. A. Eiras, Phys. Rev. B **61**, 14283 (2000).
[8] R. Guo, L. E. Cross, S. E. Park, B. Noheda, D. E. Cox, and G. Shirane, Phys. Rev. Lett. **84**, 5423 (2000).
[9] L. Bellaiche, Alberto Garcia, and David Vanderbilt, Phys. Rev. Lett. **84**, 5427 (2000).
[10] B. Jaffe, W. R. Cook, and H. Jaffe, *Piezoelectric Ceramics* (Academic, London, 1971).
[11] P. Ari-Gur and L. Benguigui, J. Phys. D **8**, 1856 (1975).
[12] W. Cao and L. E. Cross, Phys. Rev. B **47**, 4825 (1993).
[13] V. A. Isupov, Solid State Commun. **17**, 1331 (1975).
[14] E. R. Leite, M. Cerqueira, L. A. Perazoli, R. S. Nasar, Elson Longo, and J. A. Varela, J. Am. Ceram. Soc. **79**, 1563 (1996); J. C. Fernandes, D. A. Hall, M. R. Cockburn, and G. N. Greaves, Nucl. Instrum. Methods Phys. Res. B **97**, 137 (1995); A. P. Wilkinson, J. Xu, S. Pattanaik, and S. J. L. Billinge, Chem. Mater. **10**, 3611 (1998).
[15] K. Kakegawa, J. Mohri, K. Takahashi, H. Yamamura, and S. Shirasaki, Solid State Commun. **24**, 769 (1977); K. Kakegawa, J. Mohri, S. Shirasaki, and K. Takahashi, J. Am. Ceram. Soc. **65**, 515 (1982).
[16] K. Kakegawa, O. Matsunaga, T. Kato, and Y. Sasaki, J. Am. Ceram. Soc. **78**, 1071 (1995).
[17] A. P. Singh, S. K. Mishra, D. Pandey, Ch. D. Prasad, and Ramji Lal, J. Mater. Sci. **28**, 5050 (1993); A. P. Singh, S. K. Mishra, Ramji Lal, and D. Pandey, Ferroelectrics **163**, 103 (1995).
[18] K. B. Thapa, M.Sc. Physics dissertation, Banaras Hindu University, 1998.
[19] A. M. Glazer, S. A. Mabud, and R. Clarke, Acta Crystallogr., Sect. B: Struct. Crystallogr. Cryst. Chem. **34**, 1060 (1978).
[20] J. Ricote, D. L. Corker, R. W. Whatmore, S. A. Impey, A. M. Glazer, J. Dec, and K. Roleder, J. Phys.: Condens. Matter **10**, 1767 (1998).
[21] Y. Matsuo and H. Sasaki, J. Am. Ceram. Soc. **48**, 289 (1965); S. S. Chandratreya, R. M. Fulrath, and J. A. Pask, *ibid.* **64**, 422 (1981); S. Y. Chen, S. Y. Cheng, and C. M. Wang, *ibid.* **73**, 232 (1990).
[22] A. M. Glazer, Acta Crystallogr., Sect. A: Cryst. Phys. Diffr. Theor. Gen. Crystallogr. **31**, 756 (1975); A. M. Glazer, Acta Crystallogr., Sect. B: Struct. Crystallogr. Cryst. Chem. **28**, 3384 (1972).
[23] H. Thomann and W. Wersing, Ferroelectrics **40**, 189 (1982).
[24] D. Viehland, J-F. Li, X. Dai, and Z. Xu, J. Phys. Chem. Solids **57**, 1545 (1996); D. Viehland, Phys. Rev. B **52**, 778 (1995); X. Dai, Z. Xu, and D. Viehland, J. Am. Ceram. Soc. **78**, 2815 (1995); Z. Xu, X. Dai, J-F. Li, and D. Viehland, Appl. Phys. Lett. **66**, 2963 (1995).